DOI 10.1007/s11141-016-9723-5
Radiophysics and Quantum Electronics, Vol. 59, No. 7, December, 2016
(Russian Original Vol. 59, No. 7, July, 2016)

FRACTAL MODEL OF A COMPACT INTRACLOUD DISCHARGE. II. SPECIFIC FEATURES OF ELECTROMAGNETIC EMISSION

S. S. Davydenko* **and D. I. Iudin**

UDC 551.594.2+537.531

We examine the features of the electromagnetic emission of a compact intracloud discharge (CID) within the framework of the fractal approach [1] described in the first part of the article. Compact intracloud discharge is considered as the result of electric interaction of two bipolar streamer-type structures previously developed in the regions of a strong electric field inside the thundercloud. To estimate the electromagnetic emission of the discharge, the complex tree-like structure of the electric currents at the preliminary and main stages of CID was represented as the sum of a relatively slowly varying large-scale linear mean component and fast small-scale constituents corresponding to the initial formation of elementary conductive channels of the discharge tree. Mean linear current of the discharge is considered as an effective source of the VLF/LF emission at both the preliminary and main stages of a CID. Electrostatic, induction, and radiation components of the electric field at different distances from the mean current are calculated taking into account specific features of both stages of the discharge within the framework of the transmission-line model. It is shown that at the preliminary stage only the electrostatic component can mainly be detected, whereas at the main stage all the above components of the electric field can be reliably measured. Dependence of the radiation electric field at the main stage on the length of the discharge channel and propagation velocity of the current front is analyzed. It is found that due to the bi-directional expansion of the current at the main stage of a CID the radiation field pulse remains narrow in a wide range of discharge parameters. The small-scale currents corresponding to the initial breakdown between the neighboring cells of the discharge domain are considered as the sources of HF/VHF radiation. It is shown that HF/VHF emission at the preliminary stage is negligible as compared to emission at the main stage. It is also established that at the main stage, first, the HF/VHF emission burst correlates well with the initial peak of the VLF/LF electric field pulse and, second, its spectrum corresponds to the power law with an exponent between -2 and -1.

1. INTRODUCTION

The electrical sources in a thundercloud, whose electromagnetic response in the far zone is a single narrow bipolar pulse having a duration of 10 to 30 μs and accompanied by an ultrahigh-power short HF burst, belong to the class of the so-called compact intracloud discharges (CIDs). The first results of observation of such discharges were published in [2]. In subsequent years, the CIDs became the subject of intense experimental and theoretical studies. Their detailed survey is given in the first part [1] of this work. A considerable volume of data accumulated to date about the CID radiation detection made it possible to statistically reliably determine the parameters of narrow bipolar pulses (NBPs) and high-frequency bursts, which are synchronous to them [3–6]. In most cases, no electrical activity has been detected in a thundercloud, neither before nor after the compact discharge. Multipoint ground-based observations of the CID

* davyd@appl.sci-nnov.ru

[1] Institute of Applied Physics of the Russian Academy of Sciences, Russia. Translated from Izvestiya Vysshikh Uchebnykh Zavedenii, Radiofizika, Vol. 59, No. 7, pp. 620–637, July 2016. Original article submitted January 25, 2016; accepted July 17, 2016.

radiation in a wide frequency band gave a possibility to localize their position in the thunderstorm with high accuracy and establish a correspondence between the CID polarity[1] and the direction of a large-scale electric field in the region of their occurrence [7, 8], and also evaluate in some cases the charge moment variation during a discharge [5, 9, 10]. Comparison of the results of multipoint observations of the compact discharge radiation and the meteorological radar data has showed that strong convection in a thundercloud is a neccesary, but not sufficient condition for the CID occurrence [11]. The detected decrease in the CID occurrence with increasing geographic latitude is attributed exactly to a fall in the convection rate in thunderclouds [12]. An important feature of compact discharges proved to be their high spatiotemporal clustering, which is more typical of the negative-polarity discharges. A significant part of CIDs was detected, as a rule, in a relatively short period of time in the region of strong convection of some mature thunderclouds [11]. Recent experiments on high-frequency interferometry of compact discharges have established a number of fine features of their structure, in particular, the velocity and trajectory of the main source of high-frequency radiation [10, 13]. Satellite observations of the high-frequency component of the CID radiation appeared an important channel of information about compact discharges. Due to reflection of the high-frequency radiation of compact discharges from the Earth's surface, the satellites detected both the direct and reflected signals forming the so-called transionospheric pulse pairs (TIPPs) [14]. Good agreement was shown between the estimates of the CID altitude according to ground-based measurements and delay time of the reflected burst of high-frequency radiation. This confirmed the assumption about the unified source of high- and low-frequency radiation in a compact discharge. We also note that in the course of the satellite observations the optical radiation of CIDs was not detected [15].

The first attempt to describe the source of the observed narrow bipolar pulses was made in [2], where the model of low-frequency radiation of ordinary lightning discharges was used to solve the inverse problem. It was assumed that the source is a current pulse propagating vertically along the conductive channel of a given length. The radiation of such a source was described in terms of the transmission-line model, which allowed the electromagnetic field to be calculated both in the far zone and near the source [16]. The origin of the current pulse and the mechanism of the conducting channel formation without a notable high-frequency radiation are not discussed in [2]. In subsequent years, such an "engineering" approach to modeling of the low-frequency CID radiation has become widespread and made it possible to determine a number of important parameters of the sources based on the accumulated experimental data. First of all, estimates of the length of the conductive channel of the discharge were obtained. The channel appeared shorter than 1 km [4]; then discharges of this type, as a matter of fact, became known as compact. Further it was found that the parameters of the CID source (rise time, peak value, and current pulse propagation velocity) are close to the appropriate characteristics of the return-stroke stage of a typical cloud-to-ground discharge [17]. Allowance for reflection of the current pulse from the ends of the conductive channel within the framework of this approach made it possible to interpret the oscillations observed in some cases in the second half-period of a bipolar pulse of the electric field in the far zone, and also estimate the length of the conductive channel and the decay rate of the source current [18, 19].

Thus, within the framework of the mentioned approach, it became possible to determine a number of important parameters of the sources, whose field corresponds to the low-frequency component of the compact-discharge radiation. However, the question about the mechanism of the formation of such sources, as well as about the nature of the high-frequency CID radiation currently does not have a clear answer (see [1] for more details). The physical models of CID proposed to date describe, as a rule, separate features of radiation and the structure of compact discharges which are mainly related to the formation of a low-frequency radiation pulse. For example, in [20] a narrow bipolar pulse of the electric field in the far zone is formed as a result of the transient processes after the instantaneous lengthening of the leader channel. The mechanism of the formation of the channel itself, and of a high-power HF radiation burst that is synchronous to the channel lengthening, are not considered in the model. In [10], on the basis of comprehensive studies of

[1] The CID polarity is the sign of the vertical projection of the ground electric field in the far zone in the first half-period of a narrow bipolar pulse. Here, we assume that the vertical projection of the upward ground field is positive.

short discharges in the thundercloud is was assumed that compact intracloud discharges are a fast positive streamer breakdown, the development of which is not preceded by an electrical activity in the thundercloud and occurs in the region of a strong electric field. This assumption conforms well to the CID high-frequency interferometry, but the issues about the origin and properties of a high-power HF burst, as well as the mechanism of the formation of a strong electric field, are outside the scope of such a model. Another well-known model of compact discharges is based on the runaway electron breakdown mechanism [21, 22]. For such a breakdown, the shape of the emerging current pulse and the wide-band electromagnetic radiation is largely determined by the energy of the cosmic rays which are the source of the seed electrons. The main difficulties of using this mechanism for the CID description include, in particular, an extremely high energy of the breakdown-initiating cosmic rays, a large extent of the avalanche, and that too high values of the intracloud electric field, which are necessary to comply with the emerging bipolar pulse of the observation field [23]. Interpretation of the high-frequency CID radiation within the framework of this mechanism also encounters a number of difficulties stipulated by the features of the directivity pattern and radiation spectrum of an avalanche of runaway electrons [24].

Relatively recently, a model based on a fractal–probabilistic description of the current system and conductive-channel dynamics of a compact intracloud discharge was proposed in [1]. A distinctive feature of this model is the presence of a preliminary stage, at which bipolar streamer-type structures accumulating, as they develop, a considerable electric discharge near their boundaries, are formed relatively slowly in a strong nonuniform electric field of the thundercloud. As a possible mechanism of the formation of a medium-scale spatially inhomogeneous structure of the electric field, a stream instability [25] with the necessary condition that heavy large particles are present in the flow of a weakly conducting cloud medium was considered. Note that the presence of such particles even in the upper layers of the well-developed thunderclouds has recently been confirmed experimentally [26]. Spatiotemporal synchronization of the streamer-type structures is due to the amplification of the electric field near the edges of the structure during its development, which has a significant effect on the breakdown probability at the field maxima that are closest to the structure axis. The beginning of the main stage of a CID corresponds to the appearance of an electrical contact between the streamer-type structures, and the charge accumulated at their adjacent ends is neutralized over a time much less than the duration of the preliminary stage of a CID. As was mentioned in [1], the parameters and structure of the discharge currents at the preliminary stage suggest their weak electromagnetic radiation, and the key parameters of the mean current pulse formed at the main stage of a discharge are in good agreement with the known estimates obtained earlier in the transmission-line model. This paper is devoted to a detailed description of the low- and high-frequency electromagnetic radiation of a CID in terms of the model [1].

2. COMPACT-DISCHARGE STRUCTURE FORMATION AND EFFECTIVE SOURCES OF LOW- AND HIGH-FREQUENCY RADIATION

According to model [1], the CID is a dynamic hierarchical structure of conductive channels, whose evolution, properties, and currents differ considerably at the preliminary and main stages of a discharge. The description of both stages is based on an analysis of the electric charge of an elementary spatial cell of size of $10\times10\times10$ m. Variations in the cell charge at each step of the model time are due to the appearance or disappearance of the conductive channels connecting the cell and its nearest neighbors. The concept of a conductive channel was introduced in the model to describe the effective conductivity of an electrical link between the neighboring cells. For example, at the preliminary stage of a CID this link may represent a set of streamer channels or a conductive low-current structure such as the recently discovered stalkers [27]. Note that the important question about the fractal dimension of such a link, which is closely related to its electrical characteristics, requires separate analysis and is outside the scope of this paper. The probability of the occurrence of a conductive channel depends on the strength of the electric field between the neighboring cells and is described by the Weibull distribution. The electric field is the sum of the given external field and the fields of all elementary cells of the calculation domain (see [1] for more details). After the preliminary

breakdown, the electric field at the ends of the emerging elementary conductive channel is amplified due to the charge transfer between the cells during their potentials equalization, which increases the probability of the subsequent breakdowns and ensures the further discharge increase. An important feature of the conductive channels is that their lifetime depends on the current flowing therein: the higher the current flowing in the channel (and, correspondingly, the ohmic heating of the channel), the longer the time of existence of the conducting link. As a result, a tree-like bipolar hierarchic structure[2] of the conductive channels is formed with the time in the region of a strong electric field. The current is the maximum in the central, most stable part (trunk) of the discharge, while the branching periphery of the discharge (crown and roots) is formed by the rapidly varying small-scale current segments.

The discharge evolution scheme presented above is true both at the preliminary and the main stages of a CID, but the rate of variation of the discharge structure and the emerging currents differ significantly, which is due to the different mechanisms of the conductive channel formation. According to model [1], effective conductivity of the channel at the preliminary stage of a discharge is provided by streamer-type discharges, whose propagation velocity is assumed equal to $5 \cdot 10^5$ m/s [28]. The ratio between the size of an elementary cell and the discharge propagation velocity determines the step of the model time at the preliminary stage, which in this case is equal to $\tau = 20$ μs. The dynamics of the inverse resistance (conductivity) per unit length G of such a streamer channel in the model is described by the equation

$$\frac{\partial G}{\partial t} = \eta E^2 G - \beta G, \tag{1}$$

which is a differential counterpart of the Rompe–Weizel formula for the long-spark conductivity in a gas[3] [29, 30]. The first and second terms on the right-hand side of Eq. (1) describe the influence of, respectively, the ohmic heating and cooling of the channel on its conductivity. Equation (1) is used for $G > G_0$, where $G_0 = 10^{-5}\,\mathrm{S \cdot m}$ is the initial value of the inverse resistance per unit length. The channel disappears once the conductivity reduces to a certain threshold value close to G_0.

The choice of the value of G_0 can be qualitatively substantiated as follows. Suppose that the emerging channel in each cross section is a set of N co-directed streamers with the radius r_{st} and length L_{st}. The charge transfer in each streamer channel is provided by the motion of a compact head of the streamer with the characteristic velocity v_{st}. According to [28], the conductivity of the head can be estimated as $\sigma^{(\mathrm{h})}\,[\mathrm{S/m}] = 10^{14} n_e\,[\mathrm{cm}^{-3}]/p\,[\mathrm{atm}]$, where $n_e \approx 10^{14}\,\mathrm{cm}^{-3}$ is the electron number density in the streamer head [31] and p is the air pressure. Assuming that the streamer is formed at an altitude of about 12 km, we obtain $\sigma^{(\mathrm{h})} \approx 4$ S/m. The electric charge transferred by the head of one streamer is equal to $\delta q^{(\mathrm{h})} = j^{(\mathrm{h})} S_{\mathrm{st}}\,\Delta t = \sigma^{(\mathrm{h})} E S_{\mathrm{st}}\,\Delta t$, where $S_{\mathrm{st}} = \pi r_{\mathrm{st}}^2$ is the cross-sectional area of the streamer, $\Delta t = 2r_{\mathrm{st}}/v_{\mathrm{st}}$ is the time for which a streamer head with the characteristic length $2r_{\mathrm{st}}$ passes through some cross section, and E is the external electric field. On the length a of the model conducting link, a/L_{st} streamers can simultaneously be formed; therefore, at each step of the model time $\tau = L/v_{\mathrm{st}}$ such a composite single streamer channel will provide the transfer of a charge of the order of $\delta q^{(\mathrm{h})} a/L_{\mathrm{st}}$. Correspondingly, a beam of N channels at each step of the model time will provide the transfer of the charge

$$\delta Q^{(\mathrm{h})} = N \frac{a}{L_{\mathrm{st}}} \delta q^{(\mathrm{h})} = N \frac{a}{L_{\mathrm{st}}} \frac{2\pi r_{\mathrm{st}}^3}{v_{\mathrm{st}}} \sigma^{(\mathrm{h})} E.$$

Since the mean initial current $I_0 = \delta Q^{(\mathrm{h})}/\tau$ in the channel is related to the inverse resistance per unit length

[2] Note that the discharge structure at the preliminary stage of a CID can, generally speaking, differ from the tree-like one and be a set of relatively low-current small-scale streamer discharges occurring over the entire region of a strong electric field. The transition to the leader stage in the trunk of each discharge does not occur due to the smallness of the current flowing in the channel. A similar assumption on the distributed structure of the discharge current, but at the main stage of a CID, was proposed in [10].

[3] Note that the electric properties of an extended streamer channel have insufficiently been studied to date, and therefore the use of a relatively simple equation (1) for description of its conductivity dynamics is quite justified.

$I_0 = G_0 E$, we obtain

$$G_0 = N \frac{2\pi r_{\rm st}^3}{L_{\rm st}} \sigma^{(\rm h)}.$$

Assuming that $r_{\rm st} = 4 \cdot 10^{-4}$ cm (cf. [32]), the characteristic length of a streamer at the discharge altitudes $L_{\rm st} = 1$ m [28], $N = 10^4$ [33], we obtain an estimate for the initial link conductivity $G_0 \sim 10^{-5}\,{\rm S} \cdot {\rm m}$ corresponding to that adopted in the model [1].

The channel heating efficiency parameter η is assumed equal to $10^{-8}\,{\rm m}^2/(V^2 \cdot {\rm s})$, and the characteristic time of the channel conductivity dissipation is $\beta^{-1} = 0.1$ ms, which corresponds to five steps of the model time. For the chosen values of η and β, evolution of the channel conductivity leads to a relatively slow (with characteristic time of the order of ten milliseconds) formation of bipolar streamer structures at the preliminary stage of a CID [1]. In this case, as was mentioned, the emerging current system is hierarchic: the discharge periphery is formed by small-scale low-current elements with a short lifetime, and as the discharge moves towards the trunk, the lifetime of the elements and the current flowing in them increase significantly due to the summation of the currents of individual channels at the branching points. Besides, as the discharge is formed, a significant electric charge is accumulated at the preliminary stage near the ends of the discharge, and this charge provides the equipotentiality of the central, well-conducting segment of the discharge tree. It is important to note that the maximum conductivity of the channels at the preliminary stage of a CID is mainly determined by the parameter η and, in order of magnitude, does not exceed $3 \cdot 10^{-3}\,{\rm S} \cdot {\rm m}$, which corresponds to the conductivity $10\,{\rm S/m}$ for the conductive channel radius 1 cm.

A similar structure of the currents also exists at the main stage of a CID, the start of which corresponds to the instant of occurrence of an electrical contact between the bipolar streamer-type structures that formed at the preliminary stage. However, the mechanisms of the conductive channel formation at the preliminary and main stages of a CID are different. At the main stage, the breakdown occurs in a medium with pre-ionization and a considerably disturbed electric-charge distribution in a strong electric field; thus, as the mechanism of the conductive channel formation, one can consider the ionization wave, similar to the return stroke of a cloud-to-ground discharge. As at the return-stroke stage, a basic feature of the ionization wave at the main stage of a CID is the fact of an abrupt (by orders of magnitude) reduction of the discharge channel resistance per unit length after the passage of the wave front, which is a consequence of the heating, ionization, and gas-dynamic expansion of the air. For a theoretical description of this complex process, rigorously speaking, it is necessary to solve a self-consistent problem of propagation of the electric wave along the channel axis with allowance for the radial spread of the gas and its ionization in each cross section of the channel. Such a problem is extremely complicated, and is not resolved at present even for the main stage of the lightning stroke [34]. The dependence of the wave velocity on the pre-ionization level of the propagation channel is also an open question. A typical velocity of the wave front (current pulse) in the return stroke lies in the range $(1/3–2/3)c$ [35], where c is the speed of light. This is in good agreement with the estimates of the pulse propagation velocity at the main stage of a CID, which were obtained within the framework of the transmission-line model [4, 17]. In the case of a CID, the pre-ionization level of the channels is much lower than in the return stroke, but as the wave front propagates towards the center of the streamer-type structures, the channel ionization level increases, which may lead to a rise in the current pulse velocity. This issue requires special study. Here, we assume that the ionization wave propagation velocity is $5 \cdot 10^7$ m/s, which determines the step of the model time at the main stage: 0.2 μs. The ionization wave propagates up and down from the contact point; the emerging channel is considered a good conductor, so that the electric potential of the emerging conductive structure is equalized in several steps of the model time. Strong current in the channel us due to a rapid pick-up of charges of the elementary cells the channel passes through, the total charge of the channel tending to zero. The potential of the upper and lower conductive streamer-type structures is retained before the upper and lower front, respectively, of the ionization wave. The transition region of the ionization wave front, at which the main potential difference occurs, is about ten meters long, which corresponds to the chosen size of an elementary cell of the calculation domain. An important feature of the discharge channel at the main stage of a CID is its active branching in the regions

with a high charge density formed at the preliminary stage.

In the analysis of electromagnetic radiation at both stages of the CID it should be natural to assume that a relatively low-frequency component of radiation of the current system is determined by its large-scale, slowly varying segment formed by the channels with high current. The radiation of such a segment can conveniently be calculated by considering as the source the effective linear current obtained by addition of all elementary discharge currents in each horizontal plane. Fluctuations of such a total current are effectively averaged due to a large number of elements. Conversely, high-frequency radiation of a CID should be related to the initial electric breakdown of the gaps between the neighboring cells, i. e., the occurrence of new conductive channels. The characteristics of high-frequency radiation are determined by the length and spatial orientation of the discharge gap, propagation velocity, and current pulse shape in a breakdown. From this, in particular, it should be expected that the higher-frequency components of the radiation at the preliminary and main stages of a CID are significantly different.

Using the above-described presentation of current systems at the preliminary and main stages of a CID in the form of a set of effective sources of low- and high-frequency radiation, we consider specific features of the electromagnetic field of a CID in more detail.

3. ELECTROMAGNETIC RADIATION AT THE PRELIMINARY STAGE OF A COMPACT INTRACLOUD DISCHARGE

At the preliminary stage of a CID, two bipolar streamer-type structures located near one vertical axis develop almost synchronously at two neighboring maxima of a nonuniform electric field. For estimation of their electromagnetic field, we will make use of the results of calculations of the currents of such structures presented in [1].

As was mentioned above, the low-frequency radiation of this structure is provided by long-lived large-scale currents, whose spatiotemporal distribution can conveniently be represented in the form of a linear mean current aligned with the axis of the discharge structure.[4] Having integrated the discharge current density over the transverse coordinate (in the discrete representation, this corresponds to the addition of projections of the elementary currents of a discharge tree on the vertical axis z), we obtain the mean linear large-scale current $i_{\rm ps}^{\rm (I)}(z,t)$ of one bipolar structure at the preliminary stage of a discharge. Due to the addition of a large number of relatively weak small-scale currents, the spatiotemporal profile of the total current is sufficiently smooth (see Fig. 1*a*), and the current itself is directed along the vertical axis. Assuming that the discharge starts at the instant $t = 0$, the obtained mean linear current can be approximated by the analytical expression

$$i_{\rm ps}^{\rm (I)}(z,t) = I_{\rm ps}^{\rm (I)}(t) \exp\left[-\frac{|z - z_{\rm ps}^{\rm (I)}|^\gamma}{(v_{\rm ps}t)^\gamma} - \frac{|z - z_{\rm ps}^{\rm (I)}|^\gamma}{z_0^\gamma}\right], \tag{2}$$

where $z_{\rm ps}^{\rm (I)} = 12.5$ km and $2z_0 = 100$ m are the altitude of the center of the first (lower) discharge structure and its maximum vertical scale, respectively, $v_{\rm ps}$ is the rate of expansion of the discharge domain along the vertical axis, which cannot exceed the propagation velocity of the streamer (see [1]), and is approximately equal to it in the case considered: $v_{\rm ps} \lesssim 5 \cdot 10^5$ m/s, $\gamma = 6$ is the parameter of the thickness of the transition layer at the boundary of the mean-current region. The first term in the exponent in Eq. (2) describes the expansion of the current region up and down from the discharge center with the velocity $v_{\rm ps}$, up to the discharge boundaries determined by the profile of the external electric field. The time factor in Eq. (2) has the form

$$I_{\rm ps}^{\rm (I)}(t) = \begin{cases} 0, & t < 0; \\ I_{\rm ps\,0}^{\rm (I)} \exp[-(t - \tau_{\rm ips}^{\rm (I)})^2/(\tau_{\rm ps}^{\rm (I)})^2], & t \geq 0, \end{cases} \tag{3}$$

[4] By virtue of the considerable altitude of the discharge, the influence of its horizontal structure on the electromagnetic field distribution is small, which was confirmed by the results of 3D simulation; therefore, the transition to a linear current for description of the discharge fields seems quite justified.

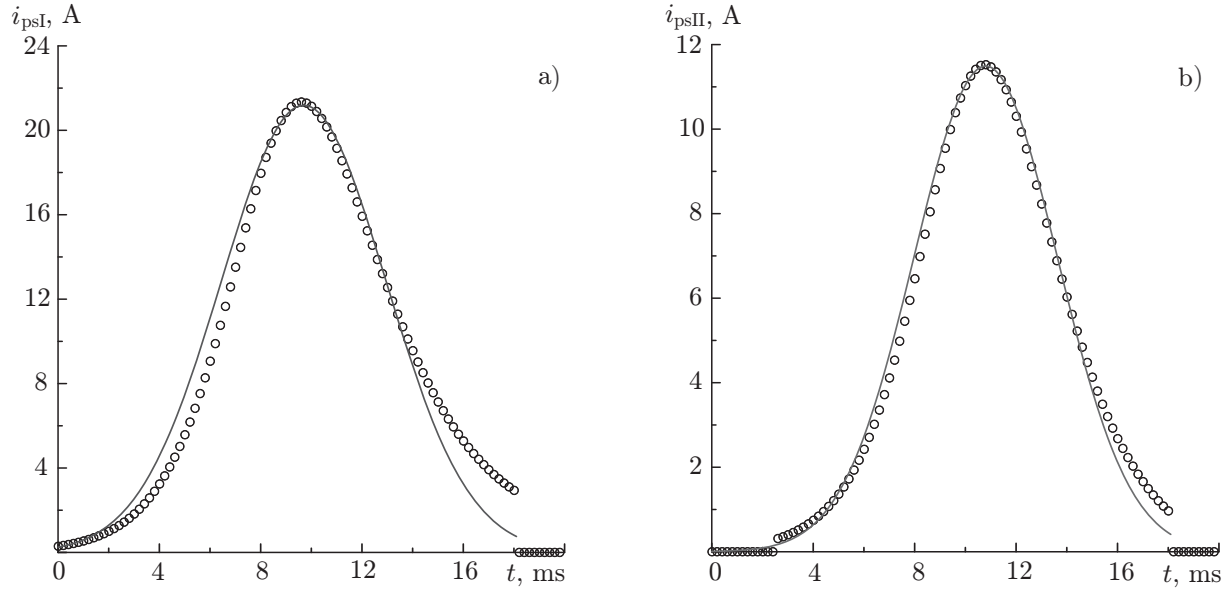

Fig. 1. Comparison of the temporal profiles of the mean linear current at the altitudes of the centers of the lower (*a*) and upper (*b*) discharges at the preliminary stage of a CID (the symbols ∘) and analytical approximation of form (3).

where $\tau_{\mathrm{ips}}^{(\mathrm{I})} = 9.7 \cdot 10^{-3}$ s and $\tau_{\mathrm{ps}}^{(\mathrm{I})} = 4.6 \cdot 10^{-3}$ s are the time of the maximum and the characteristic duration, respectively, of the mean current, and the parameter $I_{\mathrm{ps}\,0}^{(\mathrm{I})} = 21.2$ A determines the maximum current of the first discharge structure. A similar approximation can be obtained for the current of the second (upper) structure, for which $z_{\mathrm{ps}}^{(\mathrm{II})} = 12.35$ km, $\tau_{\mathrm{ips}}^{(\mathrm{II})} = 10.8 \cdot 10^{-3}$ s, $\tau_{\mathrm{ps}}^{(\mathrm{II})} = 4 \cdot 10^{-3}$ s, $I_{\mathrm{ps}\,0}^{(\mathrm{II})} = 11.5$ A. Note that the second structure appears more than 2 ms later than the first one. The use of approximations (2) and (3), on the one hand, significantly simplifies calculation of the electromagnetic field of a discharge, and on the other hand, permits one to estimate the influence of the discharge parameters on its field. Using this approximation, it is easy to calculate that the electric charge transferred over the time of existence of the first and second structures at the preliminary stage of a discharge amounts to $Q_{\mathrm{ps}}^{(\mathrm{I})} = \int_0^\infty i_{\mathrm{ps}}^{(\mathrm{I})}(z_{\mathrm{ps}}^{(\mathrm{I})}, t)\,\mathrm{d}t \approx 0.17$ C and $Q_{\mathrm{ps}}^{(\mathrm{II})} \approx 0.08$ C, respectively. Temporal profiles of the mean linear currents at the altitudes of the centers of both structures and their approximations of form (3) are compared in Fig. 1. The corresponding spatiotemporal distribution of the approximating model current (2) for both structures is given in Fig. 2*a*. Note that the rise time of the mean current for both structures is much greater than the time of propagation of the current region to the discharge boundaries: $\{\tau_{\mathrm{ps}}^{(\mathrm{I})}, \tau_{\mathrm{ps}}^{(\mathrm{II})}\} \gg z_0/v_{\mathrm{ps}}$. Therefore, an influence of the propagation effects of a current on its electromagnetic field can be neglected by dropping the first term in the exponent on the right-hand side of Eq. (2).

For calculation of the electromagnetic field of the currents $i_{\mathrm{ps}}^{(\mathrm{I})}(z,t)$ and $i_{\mathrm{ps}}^{(\mathrm{II})}(z,t)$, we will make use of the transmission-line approximation, according to which on the surface of a well conducting ground at a distance r from the axis of the vertical linear current $i(z,t)$ the vertical electric field created by the latter is described by the expression [19, 36]

$$E_z(r,t) = \frac{1}{2\pi\epsilon_0} \int\limits_{z_{\mathrm{bot}}}^{z_{\mathrm{up}}} \left\{ \frac{2z^2 - r^2}{R^5(r,z)} \int\limits_{t_{\mathrm{b}}(z)}^{t} i[z, \tau - R(r,z)/c]\,\mathrm{d}\tau + \frac{2z^2 - r^2}{cR^4(r,z)} i[z, \tau - R(r,z)/c] \right.$$
$$\left. - \frac{r^2}{c^2 R^3(r,z)} \frac{\partial i[z, \tau - R(r,z)/c]}{\partial t} \right\} \mathrm{d}z, \quad (4)$$

where ϵ_0 is the electrical constant, $z_{\rm bot}$ and $z_{\rm up}$ are the altitudes of the lower and upper boundaries, respectively, of the current region, $t_{\rm b}(z)$ is the instant at which the radiation of the current element located at the altitude z reaches the observation point at a distance r from the discharge axis, $R(r,z)=\sqrt{z^2+r^2}$ is the distance from the observation point to the point with coordinate z at the current axis, and c is the speed of light. The first, second, and third terms on the right-hand side of Eq. (4) describe the electrostatic, induction, and radiation components, respectively, of the electric field of the current $i(z,t)$. The results of calculation of the mentioned field components for the above-considered mean currents $i_{\rm ps}^{\rm (I)}(z,t)$ and $i_{\rm ps}^{\rm (II)}(z,t)$ at different distances r from the discharge axis are given in Figs. 2*b*–2*d*. It is seen that near the discharge, at $r=1$ and 10 km, the electrostatic field component which reaches 0.45 V/m is the largest, whereas the induction and radiation components, in order of magnitude, do not exceed $3\cdot10^{-3}$ and $3\cdot10^{-6}$ V/m, respectively. At a sufficiently large distance $r=100$ km from the discharge axis, all components of the field are quite small and cannot be detected in practice.

It should be noted that the electrostatic field burst at the preliminary stage of a CID is largely determined by the vertical scale of bipolar discharge structures. Elementary estimates show that the charge transferred by each structure at the preliminary stage of a CID should change proportionally to the square of its vertical size at the stage of a well-developed structure. The disturbance of the ground electrostatic field, which is determined by the dipole electric moment of the discharge structure, changes proportionally to the cube of its vertical size. Naturally, such estimates only point to the expected trend of increase in the structure-transferred charge with the increase in its vertical size z_0. A connection between these parameters in the actual systems requires a more detailed analysis. Moreover, the obtained values of the ground electrostatic field at the preliminary stage of a CID should be considered as an upper estimate since the effects related to the electrostatic shielding of the main charge of the streamer-type structure were neglected. Shielding of the main charge, especially at the late stages of evolution of a streamer-type discharge structure, can drastically attenuate its ground electrostatic field. This can be treated as an additional factor that makes the preliminary stage of a CID "invisible" when the electrical activity in the thunderclouds is detected. This issue seems important enough and will be explored elsewhere.

We now consider high-frequency radiation at the preliminary stage of a CID. As was mentioned above, the source of high-frequency radiation in our model is a current pulse that forms the conductive channel between the neighboring cells of the medium. In the calculation of the electromagnetic field it is needed to take into account spatial orientation and location of the channel, as well as the temporal profile of the current pulse and the time of its start. Therefore, the current averaging technique which was used in the calculation of low-frequency radiation is not applicable here. Note that after the appearance of the channel, the current in it varies relatively slowly, and its high-frequency radiation is small. To estimate the high-frequency radiation level, we assume that during the formation of a new, ith conductive channel between the neighboring cells, the current along the channel propagates without changing in shape: $I_i(t,r)=I_{i0}[t-(\boldsymbol{\lambda}_i\mathbf{r})/v]$, where $v=5\cdot10^5$ m/s is the current pulse velocity which we assume equal to the streamer propagation velocity $v_{\rm st}$, $\boldsymbol{\lambda}_i$ is a unit vector directed along the channel and $\mathbf{r}$ is the radius vector of the channel points. The pulse shape will be described by a linear combination of two components:

$$I_{0i}(t)=\begin{cases}0, & t<0,\quad t>L/v_{\rm st};\\ \dfrac{Q_{0i}}{\tau_2^{\rm (I)}-\tau_1^{\rm (I)}}\exp[(-t/\tau_2^{\rm (I)})-\exp(-t/\tau_1^{\rm (I)})], & 0<t<L/v_{\rm st},\end{cases}\tag{5}$$

where Q_{0i} is the total charge transferred along the ith channel at the considered step of the model time according to the model [1], the quantities $\tau_1^{\rm (I)}$ and $\tau_2^{\rm (I)}+\tau_1^{\rm (I)}$ approximately correspond to the characteristic rise and decay times, respectively, of the breakdown current pulse, which are much less than the model time step: $\tau_1^{\rm (I)}<\tau_2^{\rm (I)}\ll L/v_{\rm st}$. To calculate the electromagnetic radiation of elementary current (5) in a breakdown of the gap between the neighboring cells, we will make use of the results of [37, 38], according to which the radiation component of the electric field of such a current in the far zone on the Earth's surface

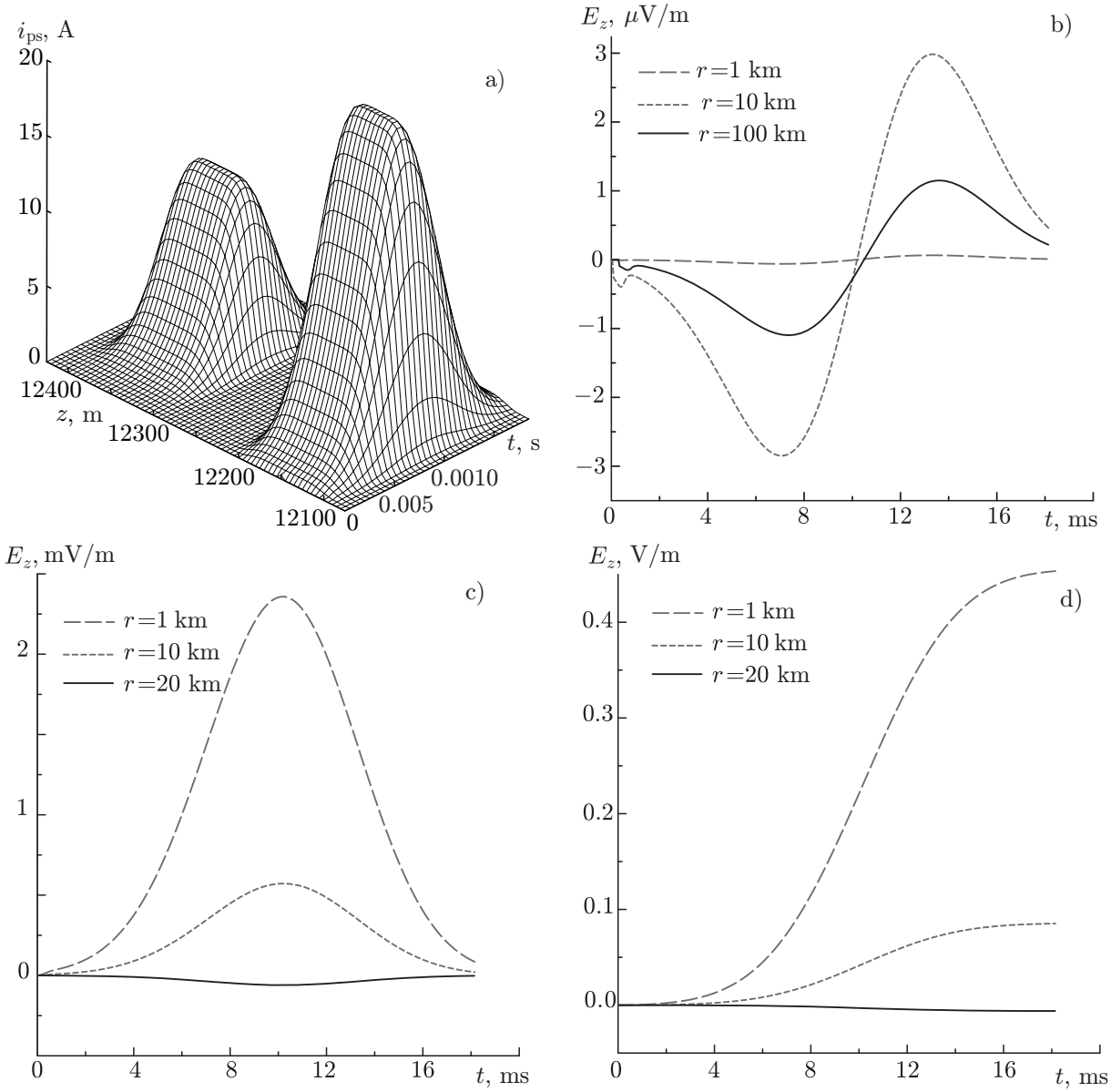

Fig. 2. Spatiotemporal distribution of linear currents of form (2), which represents the development of two streamer-type discharge structures at the preliminary stage of a CID at the altitudes $z_{\rm ps}^{\rm (I)} = 12.15$ km and $z_{\rm ps}^{\rm (II)} = 12.35$ km (*a*) and the corresponding temporal profile of the radiation (*b*), induction (*c*), and electrostatic (*d*) components of the ground electric field at different distances r from the discharge axis.

has the form

$$E_{zi}(\mathbf{r},t) = -\frac{\mu_0 v_{\rm st}}{2\pi R_{0i}} \frac{([\nabla R_{0i} \times [\mathbf{z}_0 \times \nabla R_{0i}]]\boldsymbol{\lambda}_i)}{1-(v_{\rm st}/c)\,(\boldsymbol{\lambda}_i\,\nabla R_{0i})} [I_{0i}(t-t_{{\rm a}i}) - I_{0i}(t-t_{{\rm b}i})]. \tag{6}$$

Here, R_{0i} is the distance to the center of the radiating channel, ∇R_{0i} is a unit vector along the line that connects the origin of coordinates and the center of the radiating channel, $\mathbf{z}_0$ is a unit vector of the vertical axis, $\tau_{{\rm a}i} = (\boldsymbol{\lambda}_i\,\mathbf{r}_{{\rm a}i})/v_{\rm st} + R(\mathbf{r},\mathbf{r}_{{\rm a}i})/c$, $\tau_{{\rm b}i} = (\boldsymbol{\lambda}_i\,\mathbf{r}_{{\rm b}i})/v_{\rm st} + R(\mathbf{r},\mathbf{r}_{{\rm b}i})/c$, $\mathbf{r}_{{\rm a}i}$ and $\mathbf{r}_{{\rm b}i}$ are the radius vectors of the start and the end of the ith conductive channel, $R(\mathbf{r}_1,\mathbf{r}_2)$ is the distance between the points $\mathbf{r}_1$ and $\mathbf{r}_2$, and μ_0 is the magnetic constant. Summing expressions (6) for all discharges occurring at each step of the model time, one can calculate the ground electric field at an arbitrary distance from the discharge.

A sample temporal profile of the high-frequency electric field at the preliminary stage of the considered

CID at a distance of 100 km from the discharge is shown in Fig. 3. It is seen in this figure that the amplitude of the high-frequency component of radiation at the preliminary stage of a CID is much lower than the detection threshold in the known experiments.

4. ELECTROMAGNETIC RADIATION AT THE MAIN STAGE OF A COMPACT INTRACLOUD DISCHARGE

The start of the main stage of a CID corresponds to the time of the electrical contact of the bipolar streamer-type structures formed at the preliminary stage. The discharge develops in a medium with the existing conductive channels and sharply inhomogeneous distribution of the space-charge density. Near the point of contact of the conductive structures of different polarity, the electric field increases abruptly, which, as was mentioned above, may lead to the formation of an ionization wave in the channel, as this occurs at the stage of a return stroke in the cloud-to-ground discharge. Note that this analogy has a simple physical interpretation. In the case of a return stroke, the ionization wave propagates from the point of origin up to the charged cloud along the existing leader channel. The influence of the well-conducting ground on the electric field is taken into account by introduction of the opposite-sign virtual charges located under the Earth's surface mirror-symmetrically to the real charges in the atmosphere. It is easy to notice that the pattern of the ionization wave propagation at the main stage of a CID looks similar with accuracy up to the spatial scale of the phenomenon and replacement of the virtual charges by real ones, corresponding to a conjugate bipolar streamer-type structure. Due to the high velocity of the current pulse and the short time of the main stage of a CID, all the charges not involved in the current system, can be considered as stationary during the main stage. The ionization wave, which propagates up and down the contact point, is followed by a strong current that neutralizes the charges accumulated in the medium. The length of the channel with a strong current increases with double velocity of the ionization wave, while the charge and the potential of the channel tend to zero.

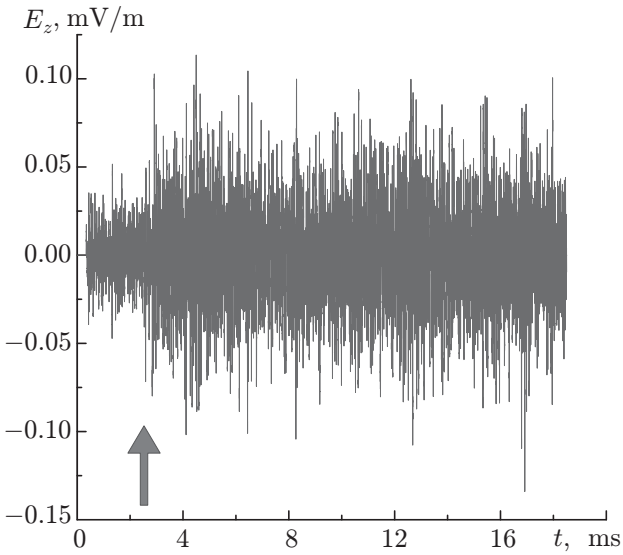

Fig. 3. Sample of the electric field of the high-frequency radiation of bipolar streamer-type structures at the preliminary stage of a CID at the distance $r = 100$ km from the discharge axis. The arrow shows the time of start of the main stage of a CID.

To analyze the electromagnetic radiation of the main stage of a CID, we will use an approach similar to that used in the Sec. 3 for describing the radiation of the preliminary stage. Assuming that the main stage of a discharge starts at the instant $t = 0$, the spatiotemporal distribution of the mean linear component of the current at the main stage of a discharge can be approximated by the expression

$$i_{\rm ms}(z,t) = I_{\rm ms}(t) \exp\left[-\frac{|z - z_{\rm ms}|^\gamma}{(v_{\rm ms}t)^\gamma} - \frac{|z - z_{\rm ms}|^\gamma}{z_0^\gamma}\right], \tag{7}$$

where $z_{\rm ms} = 12.25$ km is the altitude of the discharge center, $v_{\rm ms}$ is the rate of expansion of the discharge domain along the vertical axis, which is equal to $5 \cdot 10^7$ m/s (see Sec. 2). The time factor in Eq. (7) has the form

$$I_{\rm ms}(t) = \begin{cases} 0, & t < 0; \\ I_{\rm ms\,0} \exp[-(t/\tau_{\rm ms})^{1.1}]\{1 - \exp[-(t - \tau_{\rm ims})^{4.2}]\}, & t \geq 0, \end{cases} \tag{8}$$

where $\tau_{\rm ims}^{\rm (I)} = 1.1 \cdot 10^{-6}$ s is the rise time of the mean current, $\tau_{\rm ms} = 1.4 \cdot 10^{-6}$ s, and $I_{\rm ms\,0} = 130$ kA. As in the

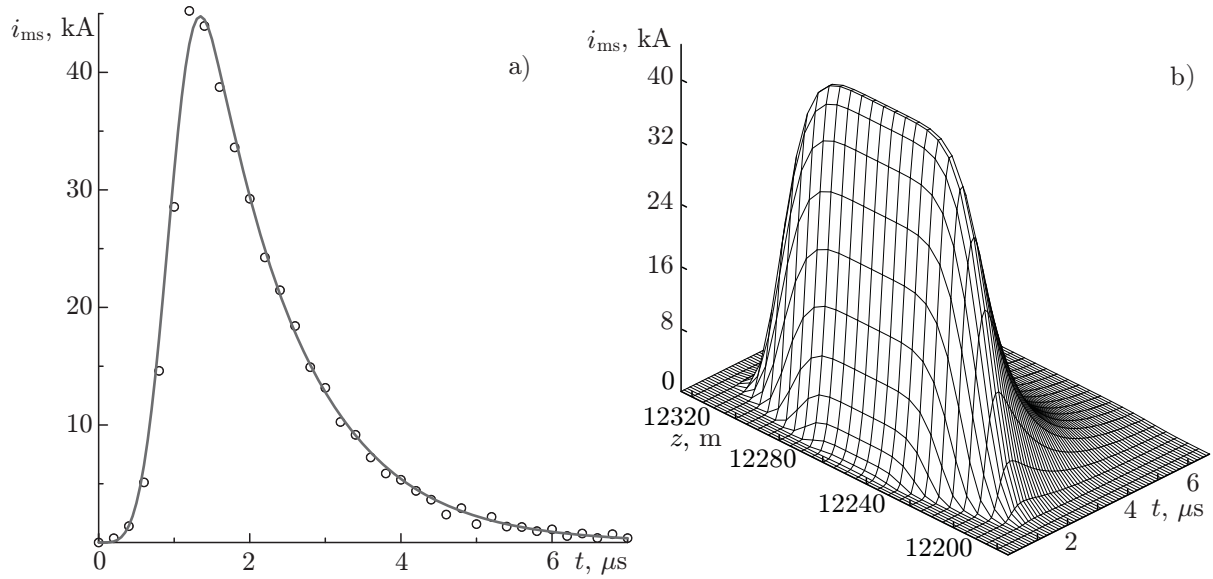

Fig. 4. Comparison of the temporal profile of current in the central channel of a discharge (symbols ∘) with analytical approximation (8) (*a*) and the spatiotemporal distribution of the mean linear current (7) (*b*) at the main stage of a CID.

analysis of radiation at the preliminary state of a CID, the use of approximations (7) and (8) considerably simplifies calculation of the electromagnetic field of a discharge. Using this approximation, it is easy to calculate that the electric charge neutralized at the main stage of a CID is $Q_{\rm ms} = \int_0^\infty i_{\rm ms}(z_{\rm ms}, t)\,{\rm d}t \approx 0.08$ C and corresponds to the charge of the smaller (upper) structure at the preliminary stage of a discharge. Calculated temporal profile of the mean linear current at the altitude of the discharge center and its approximation (8) are shown in Fig. 4*a*. Spatiotemporal distribution of the model current (7), (8) is given in Fig. 4*b*. Note that for a relatively small structure considered here, the rise time of the mean current is greater than the time of propagation of the current pulse to the discharge boundaries $\tau_{\rm ims} > z_0/v_{\rm st}$. However, the propagation effects can be significant for more extended discharges (see Sec. 4).

The electrostatic, induction, and radiation components of the field of the vertical linear current $i_{\rm ms}(z, t)$, as in Sec. 3, can be calculated in the transmission-line approximation using Eq. (4). The results of calculation of the indicated field components at different distances from the discharge axis are given in Figs. 5*a*–5*c*. Figure 5*d* shows the total field at distances of 1 and 10 km from the discharge axis.

It is seen in Fig. 5 that, unlike the preliminary stage of a CID, at short distances from the discharge axis (at $r = 1$ and 10 km) all components of the electric field give a notable contribution to the total field. Almost under the discharge, at $r = 1$ km, the induction component, which exceeds 3 V/m, dominates, while the static and radiation components amount to about 0.15 and 0.7 V/m, respectively. However, even at the distance $r = 10$ km the radiation component becomes the largest: its amplitude reaches almost 35 V/m, while the induction component decays to 0.8 V/m and the static component, in order of magnitude, does not exceed 30 mV/m. The same relation between the components is also retained at greater distances from the discharge. At $r = 100$ km, the radiation component of the field is approximately 14 V/m, in good agreement with the peak values of the field pulse of a typical CID (see, e. g., [4]). In this case, the duration of a bipolar pulse of the field is less than the typical values 10–30 μs, which is due to the extremely low vertical scale of the discharge considered. It can be expected that as the characteristic discharge length z_0 related to the scale of nonuniformity of the external electric field increases, the field pulse duration in the far zone will also increase.

As the high-frequency radiation source at the main stage, similar to the preliminary stage of a CID, we consider a set of breakdown currents of a discharge tree, which provide its increment at each step of the model time. The breakdown current which forms an elementary conductive channel between the neighboring

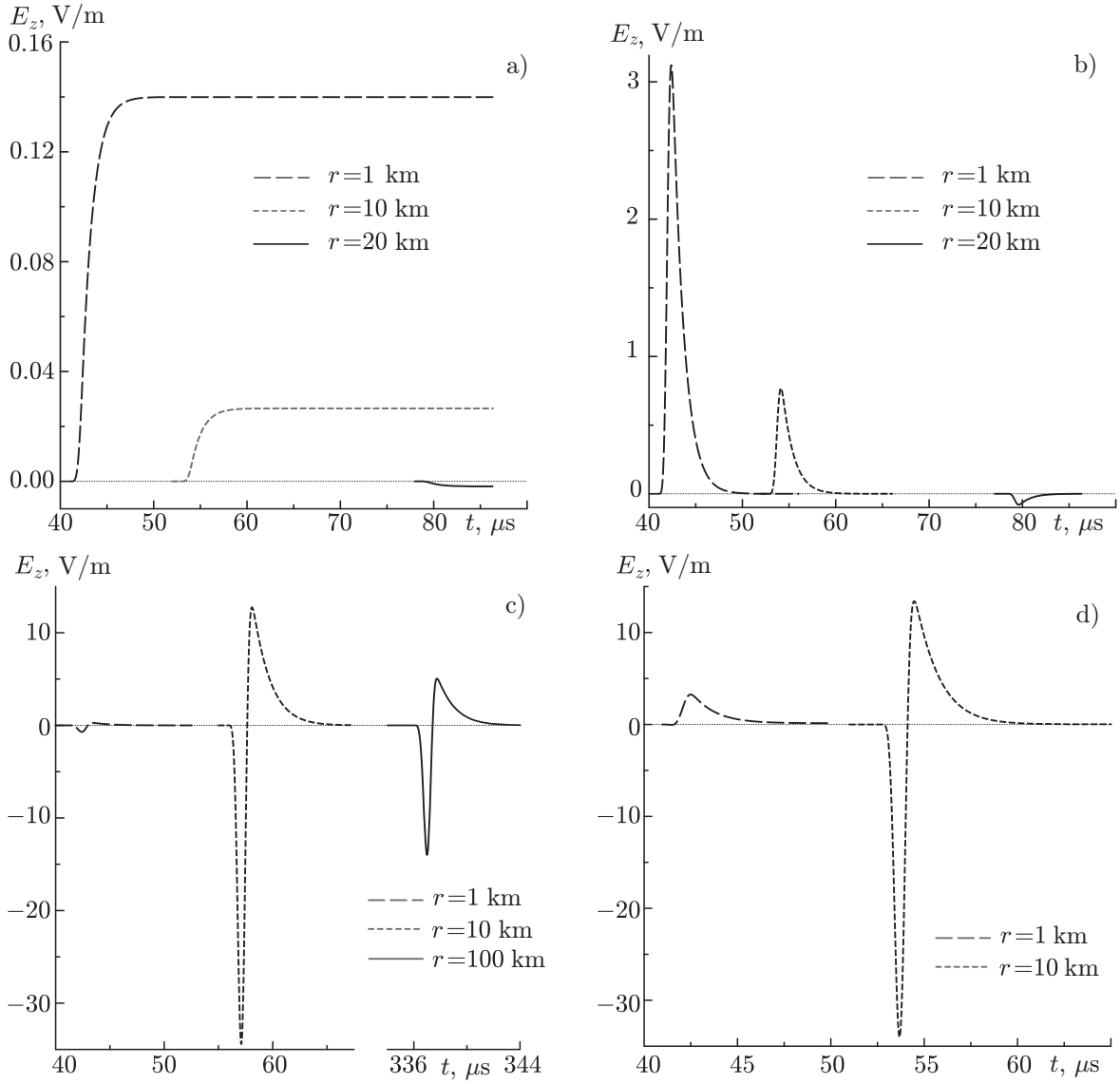

Fig. 5. Temporal profiles of the electrostatic (*a*), induction (*b*), and radiation (*c*) components of the ground electric field, as well as the total electric field (*d*) at different distances r from the main stage of the considered compact discharge centered at the altitude $z_{\rm ms} = 12.25$ km.

cells of the medium, is characterized by the coordinates and time of start, the spatial orientation $\boldsymbol{\lambda}_i$, and the temporal profile $I_i(t)$. As for the preliminary stage, we assume that the profile of the breakdown current does not change in shape during propagation along the channel. Breakdown currents at the main stage are different in that, firstly, the current pulse propagation velocity is different, $v_{\rm ms} = 5 \cdot 10^7$ m/s, and coincides with the ionization wave velocity. Secondly, the shape of the current pulse is close to the unit step function, which qualitatively describes the ionization front propagation:

$$I_{0i}(t) = \begin{cases} 0, & t < 0, \quad t > L/v_{\rm ms}; \\ \dfrac{Q_{0i}}{L/v_{\rm ms} - \tau_1}[1 - \exp(-t/\tau_1)], & 0 < t < L/v_{\rm ms}, \end{cases} \tag{9}$$

where Q_{0i} is the total charge transferred between the cells at the considered step of the model time according to the model [1] and τ_1 is the characteristic rise time of the breakdown current pulse, which is much less than the model step in time at the main stage, $\tau_1 \ll L/v_{\rm ms}$.

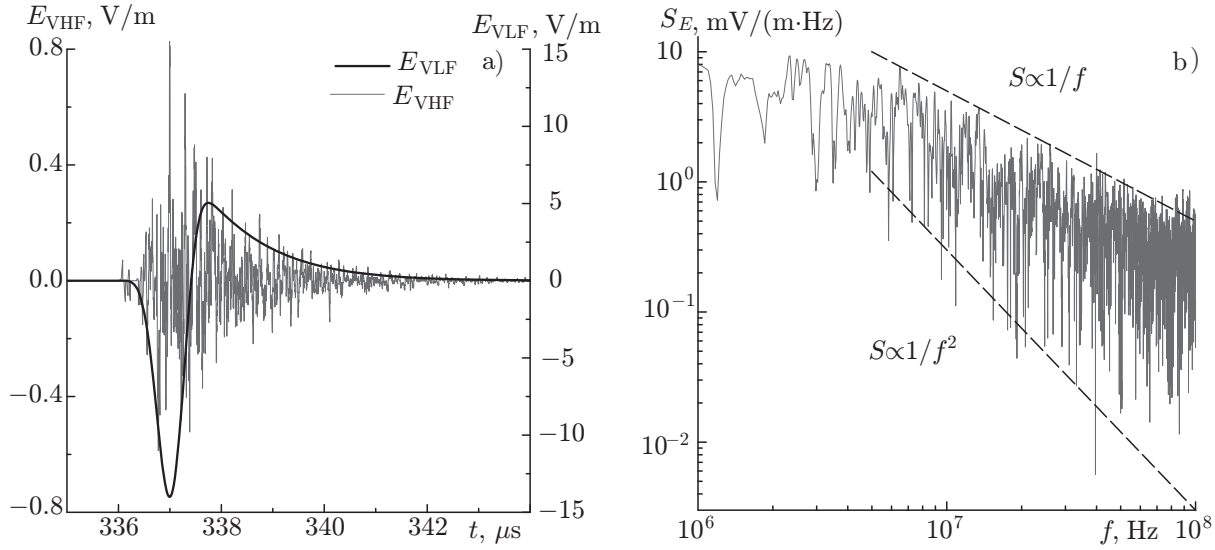

Fig. 6. Sample of the high-frerquency component of the electric field $E_{\rm VHF}$ at the main stage of a CID compared with the synchronous narrow pulse of the low-frequency electric field $E_{\rm VLF}$ (*a*) and the spectrum of the high-frequency field component (*b*) at the distance $r = 100$ km from the discharge axis.

Substituting the parameters of individual breakdown currents (9) into Eq. (6) with allowance for their start time and summing their field at each step of the model time, one can obtain the total high-frequency field at the main stage of a CID. Temporal profile of the high-frequency component of the ground electric field at the distance $r = 100$ km from the considered model discharge and its spectrum are shown in Fig. 6. It is seen that the high-frequency radiation level at the main stage of a CID is several orders of magnitude higher than at the preliminary stage (see Figs. 3 and 6*a*). In addition, Fig. 6*a* illustrates a high synchronization of the high-frequency radiation burst and a narrow bipolar pulse of the (low-frequency) electric field. The high-frequency radiation spectrum, as follows from Fig. 6*b*, lies between two power-law dependences of the form $1/f$ and $1/f^2$. The upper of the indicated boundaries corresponds to the spectrum of the process with critical dynamics and the lower corresponds to the fact that several independent realizations of such processes, whose intensity has a normal distribution, exist in the discharge.

5. CONCLUSIONS

In this paper, we present a description of the wide-band electromagnetic radiation of a compact intracloud discharge within the framework of the fractal model [1]. According to this model, a compact discharge includes a long-term preliminary stage, which is accompanied with charge accumulation by two bipolar streamer-type structures, and a short main stage, which starts in the time of electrical contact of the streamer-type structures. To describe the electromagnetic radiation of a CID, the current system at each stage of a discharge was represented as a combination of a relatively large-scale mean vertical linear current and a set of small-scale currents corresponding to the formation of new elementary conductive channels. It is shown that according to the model, only a relatively slowly rising electrostatic field component, which does not exceed a few tenths of a volt per meter for the small discharge we considered, can be detected at the preliminary stage. At the main stage of a discharge, both the electrostatic and induction field components can be detected in its close vicinity, while the radiation component, which represents a narrow bipolar pulse of the electric field and a high-power high-frequency radiation burst that is synchronous to it, dominated in the far zone. It is shown that the parameters of the electric field pulse in the far zone are in good agreement with the observations.

The proposed model has a number of features that make it different from the frequently used model in which the mean current of a CID is represented in the form of a constant-shape pulse propagating along

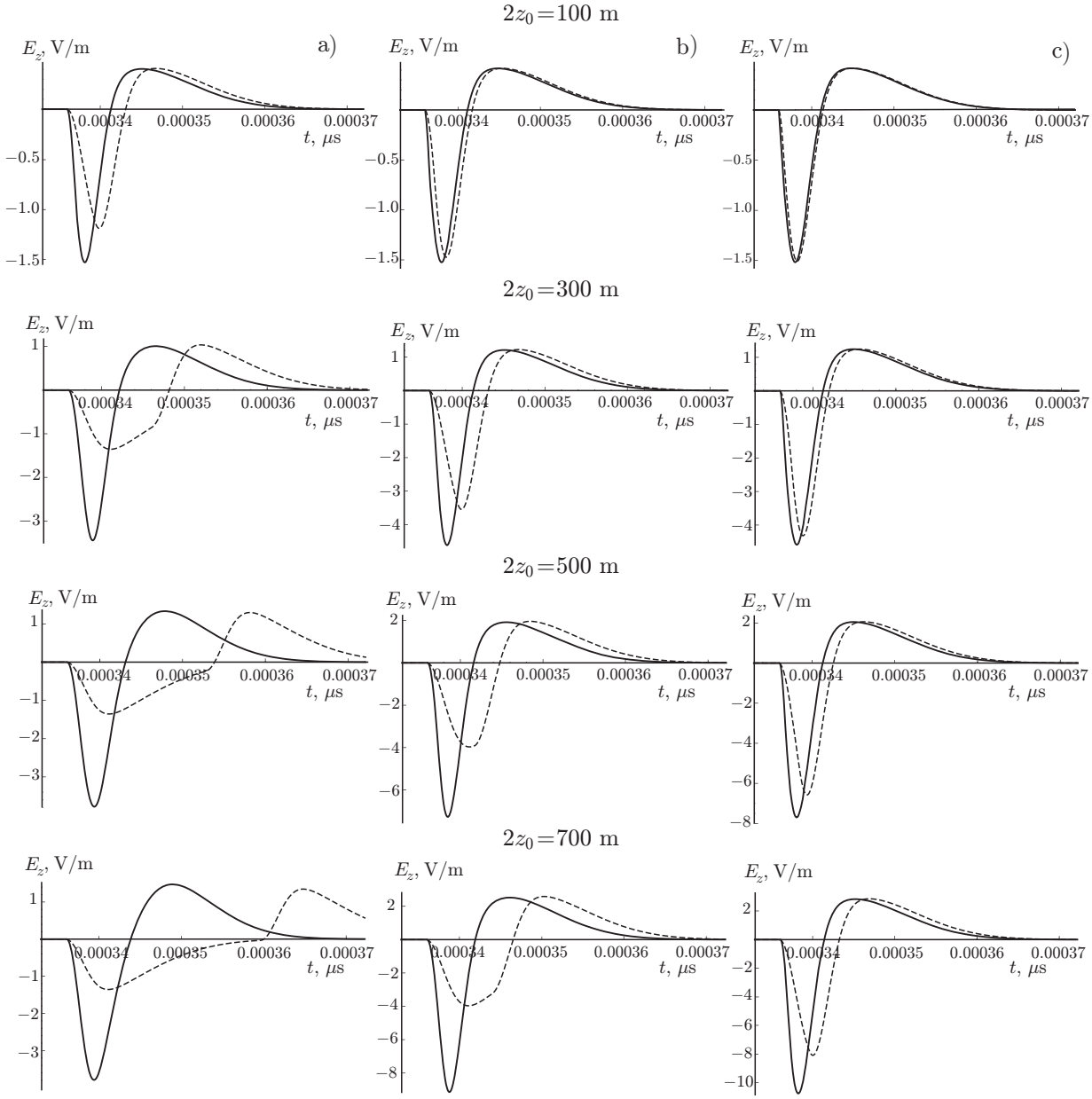

Fig. 7. Narrow bipolar pulse of the ground electric field formed at the main stage of a CID at the distance $r = 100$ km from the discharge axis as a function of the current pulse front velocity $v_{\rm ms}$ and discharge length $2z_0$. Panel (*a*) corresponds to $v_{\rm ms} = 0.1c$, (*b*), to $v_{\rm ms} = 0.3c$, and (*c*), to $v_{\rm ms} = 0.7c$. The discharge length varies from 100 to 700 m and is indicated in the figures. Solid curves correspond to the source expanding along the channel and dashed curves, to the source in the form of a traveling current pulse of constant shape.

the conductive channel. In our model, at the main stage of a discharge, the current propagates along the conductive channels simultaneously up and down from the electrical contact point of the streamer-type structures and cannot be represented in the form of a single propagating pulse. This circumstance, in particular, has a significant effect on the shape of a narrow bipolar pulse of the ground field formed in the far zone at the main stage of a CID. This effect is illustrated in Fig. 7 showing the results of calculation of the temporal profile of the electric field pulse for the expanding source (solid curves) and the source in the form of a propagating current pulse of the corresponding shape (dashed curves) for different velocities $v_{\rm ms}$ of the current pulse front and discharge length $2z_0$. It is assumed that in both cases, the lower boundary of the discharge is located at an altitude of 12 km, the pulse rise time and characteristic duration are equal to

3 and 12 μs, respectively, while the maximum discharge current is approximately 23.5 kA (see [17, 19]). It is clearly seen that for sufficiently short discharges and high velocities of the pulse front, the difference of the formed bipolar field pulses is small. However, as the discharge becomes longer and the current front velocity decreases, the bipolar field pulse, which is formed by the traveling current pulse, increasingly spreads, while it remains narrow for the expanding source. Thus, the proposed model ensures a greater stability of the shape of a bipolar field pulse compared with the model of a source in the form of a traveling current pulse, i. e., the observed narrow field pulse can be formed in a wider range of the discharge parameters.

To conclude, we note that the proposed model of a CID can in a natural way be used for interpretation of the observed narrow bipolar pulses of complex shape [6], calculation of characteristics of transionospheric pulse pairs [14], analysis of the connection of the CID and conventional lightning discharges in a thundercloud, and a number of other problems of thunderstorm electricity [5].

The authors are grateful to V. A. Rakov for fruitful discussions of the results and important comments. This work was supported by the Russian Foundation for Basic Research (project Nos. 16–05–01013 and 15–01–06612) and the Ministry of Education and Science of the Russian Federation (State contract No. 14.V25.31.0023).

REFERENCES

1. D. I. Iudin and S. S. Davydenko, *Radiophys. Quantum Electron.*, **58**, No. 7, 477 (2015).
2. D. M. Le Vine, *J. Geophys. Res.*, **85**, No. C7, 4091 (1980).
3. J. C. Willett, J. C. Bailey, and E. P. Krider, *J. Geophys. Res.*, **94**, No. D13, 16255 (1989).
4. D. A. Smith, X. M. Shao, D. N. Holden, et al., *J. Geophys. Res.*, **104**, No. D4, 4189 (1999).
5. A. Nag, V. A. Rakov, D. Tsalikis, and J. A. Cramer, *J. Geophys. Res.*, **115**, D14115 (2010).
6. S. Karunarathne, T. C. Marshall, M. Stolzenburg, and N. Karunarathna, *J. Geophys. Res. Atmos.*, **120**, 7128 (2015).
7. W. Rison, R. J. Thomas, P. R. Krehbiel, et al., *Geophys. Res. Lett.*, **26**, No. 23, 3573 (1999).
8. D. A. Smith, M. J. Heavner, A. R. Jacobson, et al.. *Radio Sci.*, **39**, No. 1, RS1010 (2004).
9. K. B. Eack, *Geophys. Res. Lett.*, **31**, No. 20, L20102 (2004).
10. W. Rison, P. R. Krehbiel, M. G. Stock, et al., *Nature Commun.*, **7**, 10721 (2016).
11. K. C. Wiens, T. Hamlin, J. Harlin, and D. M. Suszcynsky, *J. Geophys. Res.*, **113**, D05201 (2008).
12. A. R. Jacobson amd M. J. Heavner, *Mon. Weather Rev.*, **133**, No. 5, 1144 (2005).
13. H. Liu, W. Dong, T. Wu, et al., *J. Geophys. Res.*, **117**, D01203 (2012).
14. D. N. Holden, C. P. Munson, and J. C. Devenport, *Geophys. Res. Lett.*, **22**, No. 8, 889 (1995).
15. A. R. Jacobson, T. E. L. Light, and R. Nemzek, *Ann. Geophys.*, **31**, 563 (2013).
16. M. A. Uman, D. K. McLain, and E. P. Krider, *Am. J. Phys.*, **43**, 33 (1975).
17. A. Nag and V. A. Rakov, *J. Geophys. Res.*, **115**, D20103 (2010).
18. T. Hamlin, T. E. Light, X.-M. Shao, et al., *J. Geophys. Res.*, **112**, D14108 (2007).
19. A. Nag and V. A. Rakov, *J. Geophys. Res.*, **115**, D20102 (2010).
20. C. L. da Silva and V. P. Pasko, *J. Geophys. Res. Atmos.*, **120**, No. 10, 4989 (2015).
21. A. V. Gurevich, G. M. Milikh, and R. Roussel-Dupre, *Phys. Lett. A*, **165**, 463 (1992).
22. A. V. Gurevich, K. P. Zybin, and R. A. Roussel-Dupre, *Phys. Lett. A*, **254**, 79 (1999).
23. S. Arabshahi, J. R. Dwyer, A. Nag, et al., *J. Geophys. Res. Space Phys.*, **119**, 479 (2014).

24. H. E. Tierney, R. A. Roussel-Dupre, E. M. D. Symbalisty, and W. H. Beasley, *J. Geophys. Res.*, **110**, D12109 (2005).
25. V. Yu. Trakhtengerts, *Dokl. Akad. Nauk SSSR*, **308**, No. 3, 584 (1989).
26. S. M. Lazarus, M. E. Splitt, J. Brownlee, et al., *J. Geophys. Res. Atmos.*, **120**, 8469 (2015).
27. A. Y. Kostinskiy, V. S. Syssoev, N. A. Bogatov, et al., *Geophys. Res. Lett.*, **42**, 8165 (2015).
28. Yu. P. Raizer, *Gas Discharge Physics*, Springer, Berlin (1997).
29. R. Rompe, W. Weizel, *Zeitschrift für Physik*, **122**, 636 (1944).
30. A. A. Dul'zon, V. V. Lopatin, M. D. Noskov, and O. I. Pleshkov, *Tech. Phys.*, **44**, No. 4, 394 (1999).
31. S. Sadighi, N. Y. Liu, J. R. Dwyer, and H. K. Rassoul, *J. Geophys. Res. Atmos.*, **120**, 3660 (2015).
32. A. Luque, V. Ratushnaya, and U. Ebert, *J. Phys. D: Appl. Phys.*, **41**, No. 23, 234005 (2008).
33. É. M. Bazelyan and Yu. P. Raizer, *Lightning Physics and Lightning Protection*, IOP Publishing, Bristol (2000).
34. É. M. Bazelyan and Yu. P. Raizer, *Spark Discharge*, CRC Press, Boca Raton (1978).
35. V. A. Rakov, *J. Lightning Res.*, **1**, 80 (2007).
36. R. Thottappillil, V. Rakov, and M. Uman, *J. Geophys. Res.*, *102*, No. D6, 6987 (1997).
37. D. M. LeVine and R. Meneghini, *Radio Sci.*, **13**, No. 5, 801 (1978).
38. D. M. LeVine and J. C. Willett, *J. Geophys. Res.*, **97**, No. D2, 2601 (1992).